

## Article

# A Closed-Loop Biorefinery Approach for the Valorization of Winery Waste: The Production of Iron-Sulfonated Magnetic Biochar Catalysts and 5-Hydroxymethyl Furfural from Grape Pomace and Stalks

Luigi di Bitonto <sup>1,\*</sup> , Enrico Scelsi <sup>1</sup>, Hilda Elizabeth Reynel-Ávila <sup>2,3</sup>, Didilia Ileana Mendoza-Castillo <sup>2,3</sup> , Adrián Bonilla-Petriciolet <sup>3</sup> , Martin Hájek <sup>4</sup> , Ahmad Mustafa <sup>5</sup>  and Carlo Pastore <sup>1</sup> 

- <sup>1</sup> Water Research Institute (IRSA), National Research Council (CNR), Viale De Blasio 5, 70132 Bari, Italy; enrico.scelsi@ba.irsa.cnr.it (E.S.); carlo.pastore@ba.irsa.cnr.it (C.P.)
- <sup>2</sup> Consejo Nacional de Humanidades, Ciencias y Tecnologías (CONAHCYT), Ciudad de México 03940, Mexico; helizabeth\_00@hotmail.com (H.E.R.-Á.); didi\_men@hotmail.com (D.I.M.-C.)
- <sup>3</sup> Department of Chemical Engineering, Instituto Tecnológico de Aguascalientes, Aguascalientes 20256, Mexico; petriciolet@hotmail.com
- <sup>4</sup> Department of Physical Chemistry, Faculty of Chemical Technology, University of Pardubice, Studentská 95, 532 10 Pardubice, Czech Republic; martin.hajek@upce.cz
- <sup>5</sup> Faculty of Engineering, October University for Modern Sciences and Arts (MSA), 26 July Mehwar Road Intersection with Wahat Road, 6th of October, Giza 12451, Egypt; ammhamed@msa.edu.eg
- \* Correspondence: luigi.dibitonto@ba.irsa.cnr.it



**Citation:** di Bitonto, L.; Scelsi, E.; Reynel-Ávila, H.E.; Mendoza-Castillo, D.I.; Bonilla-Petriciolet, A.; Hájek, M.; Mustafa, A.; Pastore, C. A Closed-Loop Biorefinery Approach for the Valorization of Winery Waste: The Production of Iron-Sulfonated Magnetic Biochar Catalysts and 5-Hydroxymethyl Furfural from Grape Pomace and Stalks. *Catalysts* **2024**, *14*, 185. <https://doi.org/10.3390/catal14030185>

Academic Editor: John Vakros

Received: 13 February 2024

Revised: 4 March 2024

Accepted: 6 March 2024

Published: 8 March 2024



**Copyright:** © 2024 by the authors. Licensee MDPI, Basel, Switzerland. This article is an open access article distributed under the terms and conditions of the Creative Commons Attribution (CC BY) license (<https://creativecommons.org/licenses/by/4.0/>).

**Abstract:** In this work, a closed-loop strategy for the management and valorization of winery waste was proposed. The exhausted pomace and grape stalks that are typically obtained from white wine industries were used as a source of simple sugars, namely, glucose and fructose, and of lignocellulosic feedstock for the preparation of selective catalysts for the 5-hydroxymethylfurfural (5-HMF) production from fructose. A novel synthetic procedure was developed for the synthesis of iron-sulfonated magnetic biochar catalysts (Fe-SMBCs). Fourier transform infrared spectroscopy (FTIR), X-ray diffraction (XRD), scanning electron microscopy (SEM), energy-dispersive X-ray (EDX), BET surface area, porous structure analysis and determination of total amount of acid sites were performed in order to characterize the physico-chemical properties of the synthesized systems. Then, these heterogeneous catalysts were successfully tested via the dehydration of simple sugars into 5-HMF by using methyl isobutyl ketone (MIBK) and gamma valerolactone (GVL) as co-solvents. The optimum 5-HMF yield of  $40.9 \pm 1.1\%$ mol with a selectivity of  $59.8 \pm 2.6\%$ mol was achieved by adopting the following optimized conditions: 0.1 g of catalyst, volume ratio of GVL to H<sub>2</sub>O = 2 to 1, 403 K, 6 h. In addition, the catalyst was easily recycled using an external magnetic field and used for at least five reaction cycles without significant loss of catalytic activity.

**Keywords:** winery wastes; biochar; sulfonated magnetic catalysts; 5-hydroxymethylfurfural; biomass valorization; biorefinery

## 1. Introduction

### 1.1. Global Wine Production and Waste Management

Wine production is one of the most important agricultural activities in the world. According to the latest report by the International Organization of Vine and Wine (OIV) [1], global wine production was estimated at 244 million hectolitres (Mhl) in 2023. France is the largest producer, with 45.8 Mhl, followed by Italy with 43.9 Mhl and Spain with 30.7 Mhl, which together account for around 80% of the wine that is produced in Europe. Such a wine productivity generates large amounts of secondary products. It has been estimated that the processing of 100 kg of grapes generates 20–25 kg of wet solids [2], of which about 88–86% corresponds to pomace (skins and

seeds) and 12–14% to stalks [3,4]. Therefore, the management of these waste side-currents leads to environmental and economic problems [5–7]. The European Council Regulation (EC) 479/2008 on the Common Organization of the Wine Market [8] stipulates that these by-products must be sent to distilleries or to other alternative uses (e.g., spreading or composting for agronomic use or energy production by incineration). Despite their wide application, however, some aspects should be considered. In the production of distillates, large quantities of grape marc must be stored and processed in a short time to avoid the formation of undesired products, thus leading to an increase in production costs [9,10]. For white wine production, especially where pomace and stalks are immediately removed from the first squeezed grape, they must be sent to the fermentation/vinification, and the resulting residues are wet solids containing simple sugars that need to be appositely fermented into ethanol before being washed and distilled. Spreading or composting is a cost-effective and practical method of treating winery/distillery end-products [11,12]. However, such application can lead to soil and groundwater pollution due to the accumulation of heavy metals and other organic substances such as alcohols, polyphenols and organic acids [13]. Lastly, the energy generation through incineration is not considered a sustainable alternative due to the high water content in winery waste (up to 60–70%), which requires energy-intensive pre-treatments and desiccation [14]. For these reasons, there is a clear need of an alternative safer management of these residues, with the aim of their valorization for the recovery of fine chemicals and components with a high added value, according to circular economy principles.

### *1.2. Integrated Approach to Biorefinery: Development of Heterogeneous Carbon-Based Catalysts for Industrial Processes*

The design and development of an integrated biorefinery for the valorization of wine waste could offer potential benefits in terms of environmental and economic sustainability, especially if the objective of “zero-waste” discharge was achieved [15–17]. Several studies have been conducted on the valorization of winery waste through the extraction of chemical compounds [18–20] and bioactive molecules, including phenolic compounds, flavonoids, anthocyanins and stilbenes, for their antimicrobial, antioxidant and anti-inflammatory properties [21–24]. However, these components represent only 5–10% of the dry matter, not effectively solving the problem of waste disposal. The use of a pyrolytic step for the valorization of organic residues is increasingly investigated for the concomitant generation of renewable energy and biochar, which could possibly find good applications. In particular, the use of biochar as a precursor for the obtainment of specifically functionalized catalysts for the production of fine chemicals has attracted a considerable attention recently [25–27]. Biochar is an economical and environmentally friendly carbon-based material that can be produced from thermochemical degradation of biomass of various origins (e.g., agricultural waste, FORSU, sewage sludge) through pyrolysis, gasification or hydrothermal carbonization [28,29]. The surface area, porous structure and presence of oxygen-containing functional groups on the biochar surface, such as hydroxylic and carboxylic groups, have enabled its use in a wide range of applications, including the adsorption of organic pollutants and heavy metals [30,31], electrochemistry [32] and energy storage [33]. In addition, these physico-chemical properties can be further improved by activation and functionalization processes. In the field of acid catalysis, sulfonation is the most efficient method for improving the surface functionalities of biochar. Sulfonated carbon-based catalysts are obtained by direct sulfonation of biochar with sulfuric acid ( $\text{H}_2\text{SO}_4$ ) by introducing sulfonic groups ( $-\text{SO}_3\text{H}$ ) as Brønsted acid sites on the surface [34–36]. On the other hand, magnetic carbon-based materials have emerged as a sustainable alternative to facilitate the recovery of catalysts in heterogeneously catalyzed liquid-phase reactions [37–39]. At the end of the use, they can easily be recovered from the reaction medium in the presence of an external magnetic field.

### 1.3. Dehydration of Fructose for Synthesis of 5-HMF

5-Hydroxymethylfurfural (5-HMF) is one of the most promising platform molecules for the synthesis of a wide range of chemical compounds, including fine chemicals, biofuels, additives, polymers and pharmaceuticals [40,41]. 5-HMF can be produced through the dehydration of simple sugars, such as glucose and fructose, in the presence of appropriate homogeneous and heterogeneous catalysts. Homogeneous acid catalysts like mineral acids [42], organic acids [43] and ionic liquids [44] present several disadvantages, including low selectivity, corrosion of the equipment, low sustainability, high toxicity and the difficulty in the recovery of the catalyst. To overcome these problems, heterogeneous acid catalysts such as ion-exchange resins [45], metal oxides [46] and heteropoly acids [47] are currently used, because they are less corrosive and easily recoverable at the end of a reaction cycle. In this work, a closed-loop strategy for the complete valorization of winery waste was proposed. After a preliminary characterization of raw biomass wastes (grape pomace and stalks), the free simple sugars (e.g., fructose, glucose) that were present in the grape pomace were recovered using water washes. Subsequently, the exhausted washed pomace and grape stalks were subjected to pyrolysis, and the obtained biochar was used as a starting support for the synthesis of iron-sulfonated magnetic biochar catalysts (Fe-SMBCs). These new species were thoroughly characterized and used for the conversion of simple sugars (recovered using water-washing) into 5-hydroxymethylfurfural (5-HMF). The application of this innovative and sustainable approach for the management and valorization of winery waste will lead to a series of advantages, such as (i) no waste being produced, (ii) the simultaneous production of useful products (5-HMF), thus increasing the profitability of the vinification process, and (iii) the use of green and low-environmental-impact technologies for the winery waste treatment.

## 2. Results and Discussion

### 2.1. Scheme of Valorization Route: Chemical Characterization of Winery Waste

A new closed-loop valorization of fresh grape pomace, schematized as reported in Figure 1, was investigated.

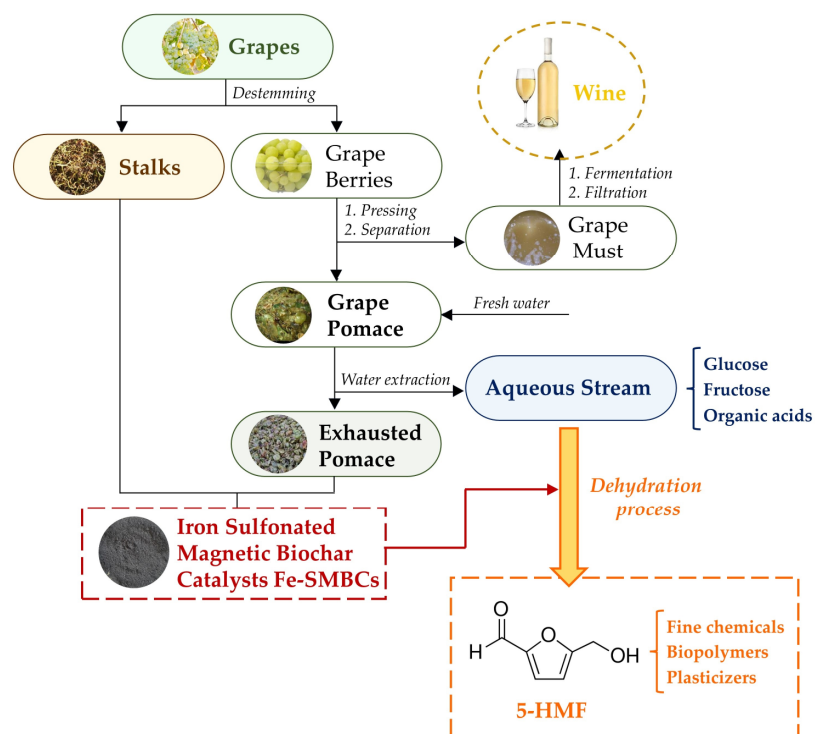


**Figure 1.** Proposed closed-loop strategy for winery waste valorization.

The scheme of valorization of fresh grape pomace is essentially based on a preliminary washing, operated with water (1:1 by weight, carried out in duplicate), with the intent of recovering simple sugars contained therein. In fact, for white wine production in particular, the fermentation appositely occurs on grape musts when it is separated from solids, which results in solids being embedded in the grape must. The results of the preliminary characterization of winery waste from the vinification process (namely, grape pomace and grape stalks) and the residues obtained after water-washing (exhausted pomace) are shown in Table 1.

**Table 1.** Chemical characterization of winery waste obtained from vinification process.

Winery Waste		Grape Pomace	Exhausted Pomace	Grape Stalks
Total Solids (TS, %wt)		67.9 ± 2.2	44.0 ± 1.4	91.8 ± 2.7
TS composition (mg/g <sub>TS</sub> )				
Total Lipids		118.8 ± 3.6	86.7 ± 2.7	19.0 ± 0.3
Free simple sugars	Glucose	30.2 ± 0.6	2.3 ± 0.1	-
	Fructose	80.6 ± 1.4	5.4 ± 0.2	-
	Total	110.8 ± 2.0	7.7 ± 0.3	-
Easy Hydrolysable Sugars (EHSs)	Arabinose	5.9 ± 0.2	8.4 ± 0.2	1.1 ± 0.3
	Glucosamine	10.6 ± 0.3	15.3 ± 0.4	-
	Galactose	18.9 ± 0.4	25.9 ± 0.7	16.1 ± 0.6
	Glucose	27.2 ± 1.1	34.7 ± 0.5	61.0 ± 1.8
	Xylose	10.0 ± 0.4	13.1 ± 0.2	77.9 ± 2.6
	Total	72.6 ± 2.4	97.4 ± 2.0	156.1 ± 5.3
Cellulose	Glucose	162.9 ± 2.7	251.7 ± 3.5	313.6 ± 4.2
	Xylose	25.1 ± 0.8	41.6 ± 0.7	31.4 ± 0.8
	Total	188.0 ± 3.5	293.3 ± 4.2	345.8 ± 5.0
Lignin		248.3 ± 6.5	277.8 ± 4.1	310.4 ± 5.1
Proteins		96.3 ± 2.1	84.9 ± 2.6	35.3 ± 1.2
Ashes		57.2 ± 1.4	69.9 ± 1.4	65.3 ± 2.1

Significant differences in chemical composition between grape pomace and stalks were determined. As well as the higher level of humidity, grape pomace is characterized by a higher content of lipids and proteins of  $118.8 \pm 3.6$  and  $96.3 \pm 2.1$  mg/g<sub>TS</sub>, respectively. In addition, free simple sugars, mainly fructose and glucose, amounting to  $110.8 \pm 2.0$  mg/g<sub>TS</sub>, are typically present in grape pomace. However, after water-washing, the simple sugar content decreased to  $7.7 \pm 0.3$  mg/g<sub>TS</sub>. These sugars were easily recovered from the grape pomace (recovery efficiency > 95%), producing an aqueous sugar stream whose composition is reported in Table 2.

**Table 2.** Chemical composition of aqueous stream obtained from extraction of free simple sugars from grape pomace.

Chemical Composition	Concentration (mmol/L)
Glucose	120 ± 0.9
Fructose	320 ± 1.6
Tartaric acid	14 ± 0.4
Malic acid	260 ± 1.4
Succinic acid	26 ± 1.0
Acetic acid	24 ± 0.7

Glucose and fructose are the major components, with a concentration of  $120 \pm 0.9$  mmol/L and  $320 \pm 1.6$  mmol/L, respectively. However, organic acids are also present, in which malic acid is the main constituent ( $260 \pm 1.4$  Mm). This aqueous stream was directly used for the subsequent dehydration tests for the production of 5-HMF. This recovery of water-soluble components makes the residual exhausted pomace richer in EHSs ( $97.4 \pm 2.0$  mg/g<sub>TS</sub>), cellulose ( $293.3 \pm 4.2$  mg/g<sub>TS</sub>) and lignin ( $277.8 \pm 4.1$  mg/g<sub>TS</sub>). In grape stalks, cellulose and lignin are the main components, with values of  $345.8 \pm 5.0$  and  $310.4 \pm 5.1$  mg/g<sub>TS</sub>. These lignocellulosic biomass wastes (exhausted pomace and grape stalks) were used as starting material for the synthesis of iron-sulfonated magnetic biochar catalysts (Fe-SMBCs).

## 2.2. Synthesis and Characterization of Iron-Sulfonated Magnetic Biochar Catalysts (Fe-SMBCs)

The conventional method for the preparation of a sulfonated magnetic carbon catalyst [48–50] generally consists of a preliminary impregnation of biochar obtained from raw biomass with an aqueous solution of iron (III) chloride or sulfate, followed by thermal activation of the impregnated biochar under a nitrogen flow (typically 773–973 K), resulting in magnetite ( $\text{Fe}_3\text{O}_4$ ) formation and deposition on the carbon-based surface. Finally, the acid functionalities are introduced on the  $\text{Fe}_3\text{O}_4$ -supported biochar by direct sulfonation with sulfuric acid ( $\text{H}_2\text{SO}_4$ ). However, this sequence of operations results in a partial loss of iron oxide after the acid treatment, adversely affecting the processes of separation and recovery of the catalyst by application of an external magnetic field. In this work, a novel synthetic procedure was developed to obtain heterogenous catalysts, in which nanostructured magnetite ( $\text{Fe}_3\text{O}_4$ ) was deposited onto sulfonated biochar that was characterized by strong acid properties. The synthetic procedure adopted for the synthesis of Fe-SMBCs is reported in Figure 2.

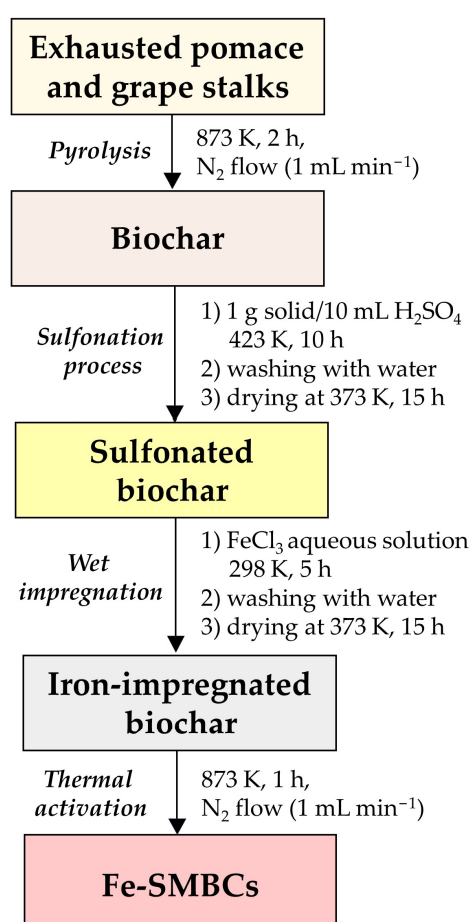


**Figure 2.** Procedure for the synthesis of Fe-SMBCs.

Firstly, biochar was produced from the pyrolysis of dried winery waste (exhausted pomace and grape stalks) at high temperatures (873 K, 2 h). This specific treatment produced a loss of weight of 71 and 73% of the original weight of the exhausted pomace and stalks, respectively. The resulting carbonaceous materials were then treated with concentrated sulfuric acid (373 K, 15 h), which led to the functionalization of the catalyst surface with sulfonic groups. FTIR analysis was performed to identify the different groups that were present in the sulfonated biochar. The FTIR spectra of raw and sulfonated biochars are shown in Figure 3. Both spectra showed similar infrared absorption bands at 3418 and  $1610\text{ cm}^{-1}$ , which are attributed to the stretching vibrations of the -OH and -COOH groups, respectively, generated during the pyrolysis process. In addition, discrete vibra-

tional frequencies at 2927 and 2850  $\text{cm}^{-1}$  should be assigned to symmetric and asymmetric vibrations of the saturated aliphatic groups. After the sulfonation process, the presence of signals at 1123 and 1100  $\text{cm}^{-1}$ , related to C-O-S and O=S=O stretching vibrations [51,52], confirmed the successful loading of  $-\text{SO}_3\text{H}$  functional groups on the native biochar surfaces.

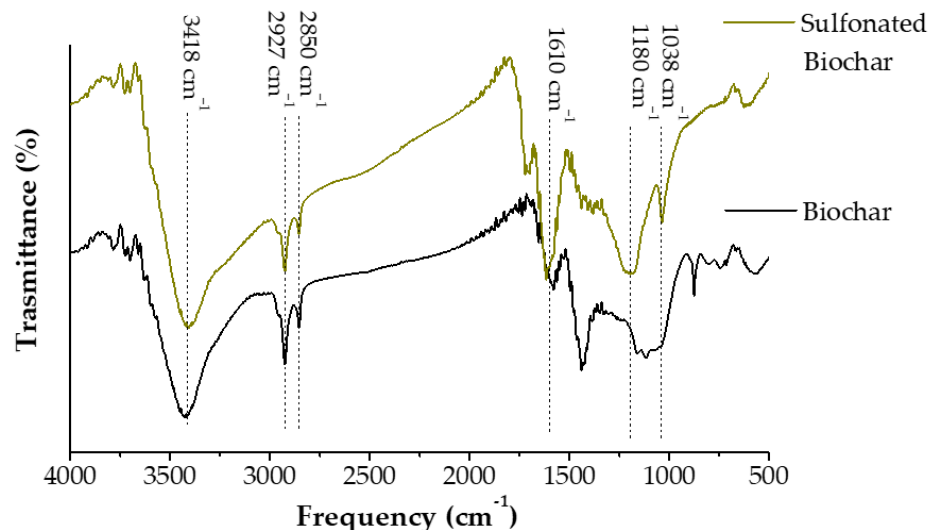


**Figure 3.** FTIR spectra of biochar and sulfonated biochar samples.

Subsequently, the sulfonated biochar was impregnated with an aqueous solution of iron (III) chloride dihydrate (298 K, 5 h) and thermally activated (873 K, 1 h under a  $\text{N}_2$  flow) in order to obtain the formation of iron-sulfonated magnetic biochar catalysts. Figure 4 shows the XRD patterns of the biochar and Fe-SMBCs obtained from the two different types of winery waste (exhausted pomace and grape stalks).

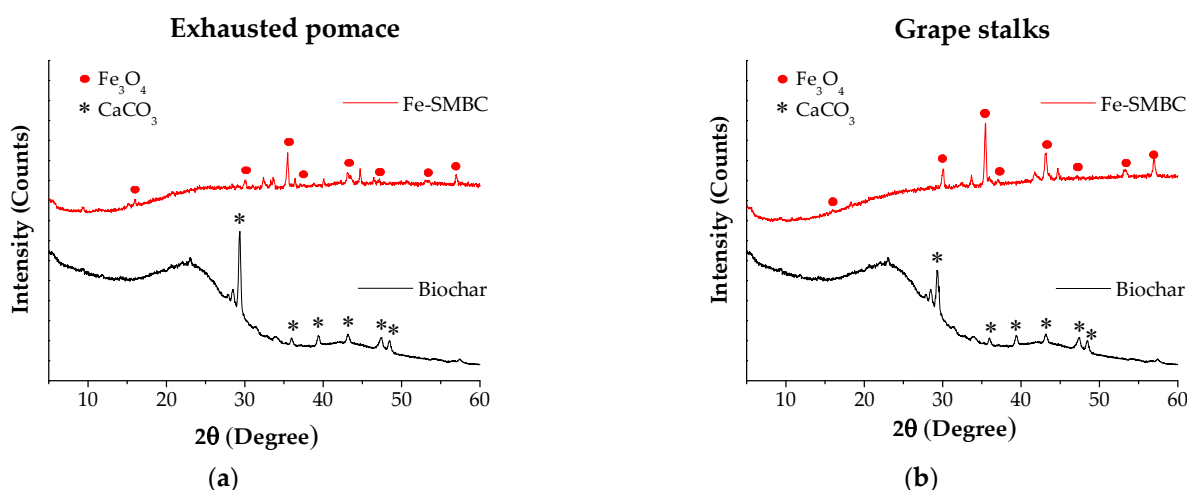
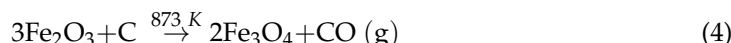
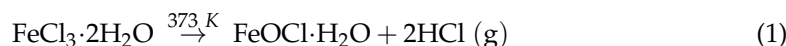


**Figure 4.** XRD patterns of biochar and iron-sulfonated magnetic biochar catalysts (Fe-SMBCs) obtained from (a) exhausted pomace and (b) grape stalks.

Signals located at  $2\theta$  of 29.3°, 35.9°, 43.0°, 47.4° and 48.5° identify the presence of calcium carbonate ( $\text{CaCO}_3$ ) in the starting biochar. A weak broad diffraction peak at  $2\theta = 23\text{--}28^\circ$  in both spectra (biochar and Fe-SMBCs) can be attributed to amorphous carbon structures with aromatic carbon layers [53]. The diffraction peaks in the Fe-SMBCs at  $2\theta$  of 16.1°, 30.2°, 35.5°, 37.7°, 43.2°, 47.5°, 53.5° and 57.1° highlight the formation of magnetite

(Fe<sub>3</sub>O<sub>4</sub>) on the catalyst, according to the reaction mechanism proposed by Bedia et al. [54] (Equations (1)–(4)):



During the drying of the iron-impregnated biochar (373 K, 15 h), FeCl<sub>3</sub>·2H<sub>2</sub>O is decomposed into the amorphous iron (III) oxide–hydroxide (FeOOH) (Equations (1) and (2)). Subsequently, FeOOH is first decomposed to iron (III) oxide (Fe<sub>2</sub>O<sub>3</sub>) as the temperature increases (873 K, 1 h) (Equation (3)) and finally reduced to form Fe<sub>3</sub>O<sub>4</sub> by reacting with the carbon surface of the catalyst. EDX analysis was used to confirm the effectiveness of the synthesis process at all stages of the preparation. Table 3 shows the elemental analyses of biochar, biochar sulfonate and Fe-SMBCs obtained from the exhausted pomace and grape stalks, respectively.

**Table 3.** Elemental analysis of biochar, sulfonated biochar and Fe-SMBCs obtained from winery waste (exhausted pomace and grape stalks).

Samples	Elemental Composition (%wt)				
	C	O	Ca	S	Fe
Exhausted pomace					
Biochar	62.6 ± 2.3	18.6 ± 2.1	0.5	-	-
Sulfonated biochar	63.3 ± 3.6	28.9 ± 2.6	0.7	5.8 ± 0.7	-
Fe-SMBCs	51.4 ± 9.4	15.4 ± 2.5	0.5	4.0 ± 0.4	18.6 ± 3.9
Grape stalks					
Biochar	75.5 ± 2.3	23.1 ± 3.3	0.5	-	-
Sulfonated biochar	61.3 ± 1.7	29.8 ± 1.2	0.9	6.8 ± 0.4	-
Fe-SMBCs	46.1 ± 1.9	15.8 ± 1.8	0.8	4.3	21.1 ± 0.4

After the sulfonation process, the chemical composition of the biochar was clearly different. The increase in sulfur (S) and oxygen (O) from 5.8 ± 0.7%wt and 6.8 ± 0.4%wt to 28.9 ± 2.6%wt and 29.8 ± 1.2%wt, respectively, indicated the successful incorporation of -SO<sub>3</sub>H groups on the biochar surfaces. The presence of iron (Fe) in the sulfonated materials after the wet impregnation, washing with water, and thermal activation was 18.6 ± 3.9%wt and 21.1 ± 0.4%wt and confirmed the formation of Fe<sub>3</sub>O<sub>4</sub> in the Fe-SMBCs. The surface morphologies of the synthesized catalysts were then studied by SEM analysis. The images obtained are shown in Figure 5. Biochar obtained from the pyrolysis of exhausted pomace (Figure 5a',a'') exhibits an irregular morphology with a well-developed pore structure, resulting from the loss of volatile compounds during the thermal treatment. A similar structure was also found for biochar obtained from grape stalks (Figure 5d',d''); however, the alveolar structure was less developed due to the higher lignin content that was present in the initial biomass (310.4 ± 5.1 mg/g<sub>TS</sub>). After the sulfonation process, a noticeable change in the surface structure of the biochar was observed in both cases (Figure 5b',b'',e',e''). A partial reduction in porosity on the surface of the carbonaceous material was obtained due to the partial removal of part of the amorphous carbon that was present in the starting biochar after the treatment with H<sub>2</sub>SO<sub>4</sub> [55,56].

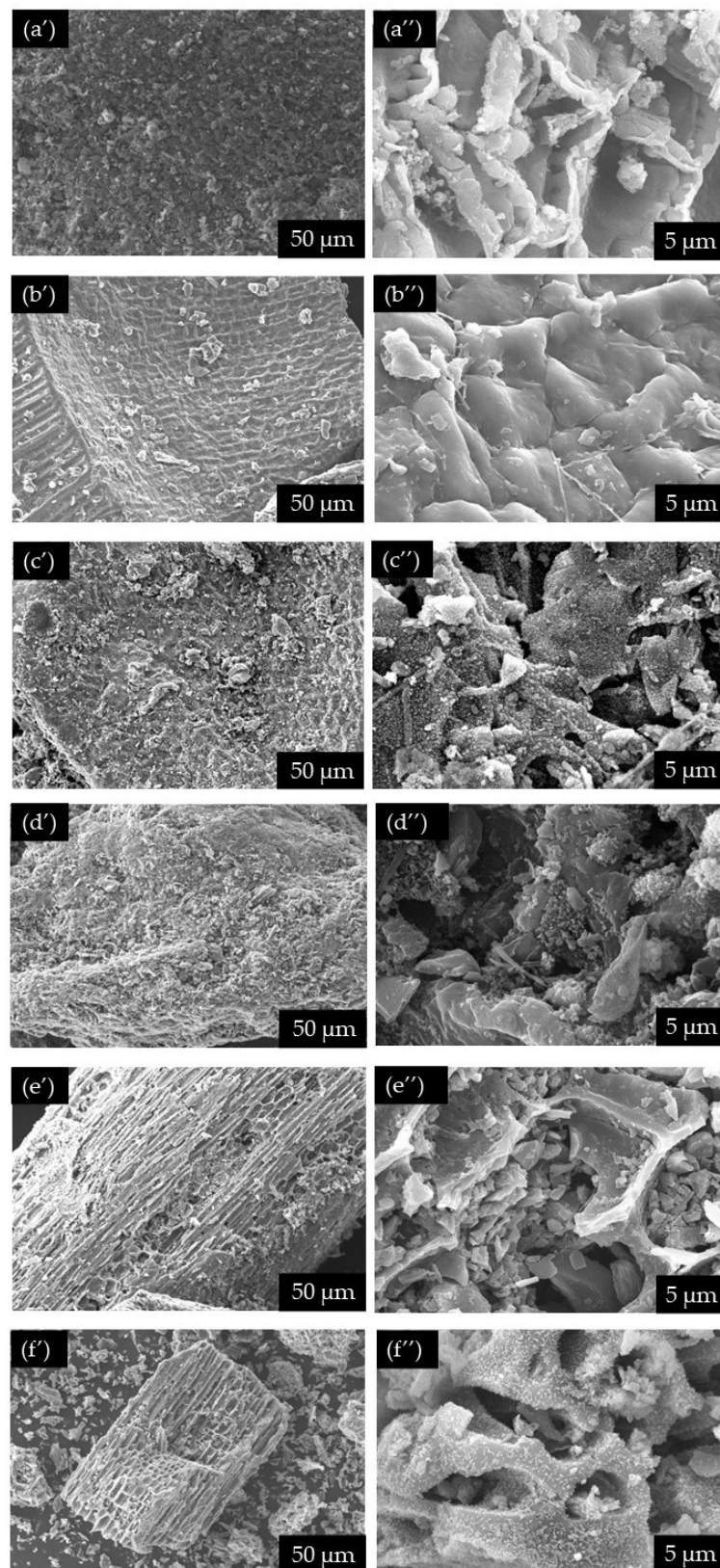


**Figure 5.** SEM images of biochar ((a',a'',d',d'') for exhausted pomace and grape stalks, respectively), sulfonated biochar ((b',b'',e',e'') for exhausted pomace and grape stalks) and Fe-SMBCs ((c',c'',f',f'') for exhausted pomace and grape stalks) at 50 and 5  $\mu\text{m}$ .

$\text{Fe}_3\text{O}_4$  nanoparticles were found on the surface of the Fe-SMBCs after the wet impregnation of the sulfonated biochar with  $\text{FeCl}_3$  and the subsequent activation process,

as confirmed by elemental EDX analysis (see Table 3). Finally, the synthesized materials were completely characterized by their BET surface area, an analysis of porosity and the determination of the total acid sites. As reported in Table 4, a partial collapse of the porous structure of the biochar obtained from the exhausted pomace and grape stalks was observed after the sulfonation process, with a reduction in the BET surface area from 6.7–17.0 m<sup>2</sup>/g to 2.5–10.4 m<sup>2</sup>/g, respectively, and pore volume from 0.039–0.029 cm<sup>3</sup>/g to 0.006–0.019 cm<sup>3</sup>/g. At the same time, an increase in the total number of acid sites was observed on the surface of the sulfonated biochar to 0.86 ± 0.01 mmol<sub>SO<sub>3</sub>H</sub>/g and 0.85 ± 0.01 mmol<sub>SO<sub>3</sub>H</sub>/g.

**Table 4.** Chemical properties of biochar, sulfonated biochar and Fe-SMBCs obtained from exhausted pomace and grape stalks.

Samples	Total Surface Area (m <sup>2</sup> /g)	Total Pore Volume (cm <sup>3</sup> /g)	Mesoporous Volume (cm <sup>3</sup> /g)	Total Acid Density (mmol <sub>SO<sub>3</sub>H</sub> /g)
Exhausted pomace				
Biochar	6.7	0.039	0.023	-
Sulfonated biochar	2.5	0.006	0.005	0.86 ± 0.01
Fe-SMBCs	4.1	0.013	0.010	0.91 ± 0.03
Grape stalks				
Biochar	17.0	0.029	0.024	-
Sulfonated biochar	10.4	0.019	-	0.85 ± 0.01
Fe-SMBCs	6.2	0.019	0.015	0.92 ± 0.02

The support of magnetite on the surface of the sulfonated biochar does not affect the acid properties of the synthesized catalysts, resulting in an overall acid density that is equal to 0.91 ± 0.03 mmol<sub>SO<sub>3</sub>H</sub>/g and 0.92 ± 0.02 mmol<sub>SO<sub>3</sub>H</sub>/g.

### 2.3. Use of Fe-SMBCs in Dehydration of Fructose for the Synthesis of 5-HMF

Fe-SMBCs obtained from exhausted pomace and grape stalks (denoted as EX and GSs, respectively) were initially tested in the dehydration of pure fructose for the synthesis of 5-HMF (Figure 6).

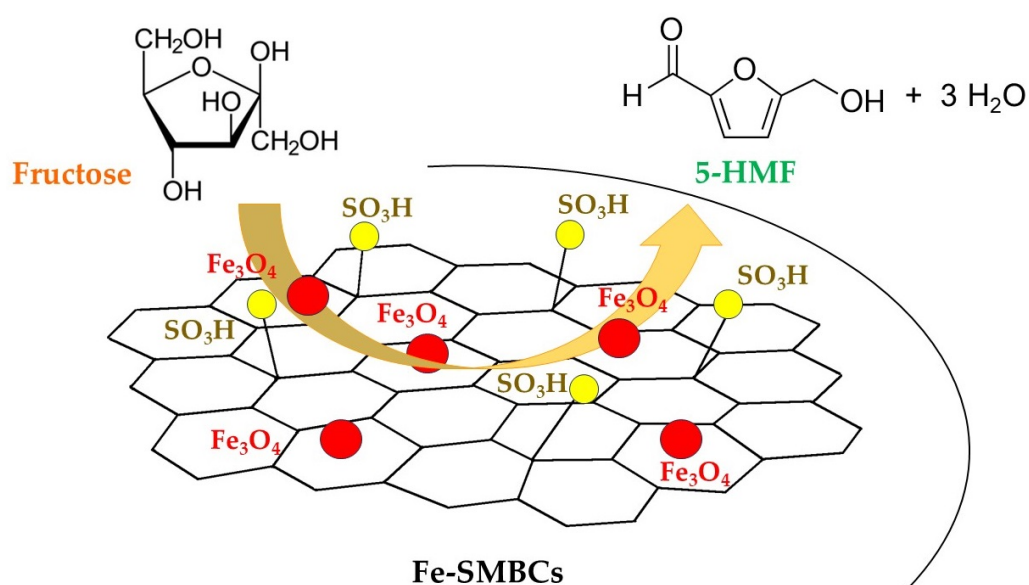


**Figure 6.** Use of Fe-SMBCs as catalysts in the dehydration of fructose for the synthesis of 5-HMF.

Although water is the most economical and environmentally friendly solvent, 5-HMF presents high instability in aqueous solutions, undergoing several side reactions that lead to the formation of oligomeric by-products (humins) [40,41]. In order to improve the yield of 5-HMF while maintaining good selectivity in the process, the dehydration reaction was conducted using methyl isobutyl ketone (MIBK) or  $\gamma$ -valerolactone (GVL) as co-solvents. In addition, the catalytic activity of the commercial sulfonic acid resins Amberlyst-15 was also investigated as a sort of reference of reactivity. The results obtained are reported in Table 5.

**Table 5.** Reactivity tests of the dehydration of fructose for the synthesis of 5-HMF. Reaction conditions: 0.1 g of catalyst, 1 mL of aqueous solution of fructose (0.2 mmol), 2 mL of organic solvent (MIBK or GVL), 403 K, 3–6 h, 300 rpm.

E	Solvent	Catalyst	Time (h)	Fructose Conversion (%mol)	5-HMF			Formic Acid	Levulinic Acid
					Yield (%mol)	Selectivity (%mol)	R	Yield (%mol)	Yield (%mol)
1		No catalyst	3	30.4 ± 0.6	4.0 ± 0.2	13.2 ± 0.9	2.0	-	-
2			6	34.7 ± 1.2	8.1 ± 0.3	23.3 ± 1.7	2.2	-	-
4	MIBK	Amberlyst-15	3	61.3 ± 2.3	8.2 ± 0.3	13.4 ± 1.0	2.2	14.2 ± 0.5	10.4 ± 0.4
5			6	91.8 ± 1.4	14.5 ± 0.5	15.8 ± 0.8	2.4	32.3 ± 1.6	28.6 ± 1.4
6		Fe-SMBCs (EX)	3	45.8 ± 0.8	5.2 ± 0.2	11.4 ± 0.6	2.0	-	-
7			6	61.2 ± 1.2	23.4 ± 0.7	38.2 ± 1.9	2.4	-	-
8		Fe-SMBCs (GSs)	6	60.1 ± 1.0	22.1 ± 0.5	36.8 ± 1.4	2.7	-	-
9			No catalyst	6	33.0 ± 0.7	5.6 ± 0.2	17.0 ± 0.9	-	-
10	GVL	Fe-SMBCs (EX *)	3	50.7 ± 1.2	20.1 ± 0.6	39.6 ± 2.1	-	-	-
11			6	72.5 ± 1.1	41.8 ± 0.8	57.7 ± 1.9	-	-	-
12			Fe-SMBCs (GSs *)	6	70.5 ± 1.2	40.8 ± 0.7	57.9 ± 2.1	-	-
	6	8.1 ± 0.4**		2.1 ± 0.1	25.9 ± 0.7	-	-	-	

\* EX = exhausted pomace, GSs = grape stalks; \*\* reaction conducted in the presence of glucose (0.2 mmol).

In the absence of a catalyst, when 0.2 mmol fructose was reacted in 1 mL of water and 2 mL of MIBK at 403 K, a conversion of  $34.7 \pm 1.2\%$ mol was achieved after 6 h, with a 5-HMF yield of  $8.1 \pm 0.3\%$ mol and a selectivity of  $23.3 \pm 1.7\%$ mol (Entry 2). When Amberlyst-15 was used as a catalyst (Entry 5), the fructose conversion was  $91.8 \pm 2.3\%$ mol with a 5-HMF yield of  $14.5 \pm 0.5\%$ mol. However, the selectivity for producing 5-HMF was found to be only  $15.8 \pm 0.8\%$ mol, which was lower than the non-catalyzed process. In particular, the Amberlyst-15 acidity was found to be strong enough to promote the subsequent hydrolysis to produce formic and levulinic acids as reaction by-products ( $32.3 \pm 1.6\%$ mol and  $28.6 \pm 1.4\%$ mol, respectively) [45]. In contrast, despite a lower fructose conversion rate of  $61.2 \pm 1.2\%$ mol– $60.1 \pm 1.0\%$ mol (Entries 7,8), Fe-SMBC showed a higher yield and selectivity towards 5-HMF production, with values in the range of  $23.4 \pm 0.7\%$ mol– $22.1 \pm 0.5\%$ mol and  $38.2 \pm 1.9\%$ mol– $36.8 \pm 1.4\%$ mol, confirming the effectiveness and the selectivity of catalysts in the dehydration process. The simultaneous presence of Brønsted (sulfonic groups) and Lewis (magnetite) acid sites effectively catalyzed the dehydration of fructose, in contrast to Amberlyst-15, which only contains sulfonic groups ( $4.3 \text{ mmolSO}_3\text{H/g}$ , experimentally detected). These values can be further improved by using GVL as a co-solvent reaction (Entries 11,12), with yields in 5-HMF of  $41.8 \pm 0.8\%$ mol– $40.8 \pm 0.7\%$ mol and selectivity of  $57.7 \pm 1.9\%$ mol– $57.9 \pm 2.1\%$ mol. In the adopted reaction conditions (volume ratio GVL:H<sub>2</sub>O = 2:1), the reaction medium becomes homogeneous. However, the use of GVL as a co-solvent limits the degradation processes of fructose and 5-HMF that lead to the formation of humic substances, thus increasing the selectivity towards the production of 5-HMF [57]. However, in the case of MIBK, a clear and convenient separation of the produced 5-HMF was achieved at the end of the process. More than 70% of the 5-HMF was easily recovered in the organic phase ( $R = 2.4$ – $2.7$ ), allowing for the subsequent isolation of the final product by distillation, with a purity greater than 90%mol [58,59]. In addition, the catalytic activity of Fe-SMBC in the direct dehydration of glucose for the synthesis of 5-HMF was measured. By adopting the same experimental conditions (Entry 13), the

yield of 5-HMF was only  $8.4 \pm 0.4\%$ mol. Lewis acid sites on the catalyst surface were not sufficient to promote the isomerization of glucose to fructose, which was subsequently converted to 5-HMF. After this preliminary investigation, in order to assess the closed-loop strategy for the management and valorization of winery waste, Fe-SMBCs were tested in the dehydration of free simple sugars that were recovered from grape pomace. The aqueous current that was recovered from washing grape pomace was directly used without any pre-treatment in the dehydration process for the production of 5-HMF (Table 6).

**Table 6.** Dehydration of the aqueous stream obtained from the recovery of free simple sugars from grape pomace for the synthesis of 5-HMF. Reaction conditions: 0.1 g of catalyst, 1 mL of aqueous solution, 2 mL of organic solvent (GVL), 403 K, 6 h, 300 rpm.

E	Solvent	Catalyst	Sugar Conversion (%mol)	5-HMF	
				Yield (%mol)	Selectivity (%mol)
1		No catalyst	$26.9 \pm 0.8$	$5.6 \pm 0.2$	$20.8 \pm 1.3$
2	GVL	Fe-SMBCs (EX *)	$69.5 \pm 1.4$	$40.7 \pm 1.2$	$58.6 \pm 2.8$
3		Fe-SMBCs (GSs *)	$68.4 \pm 1.3$	$40.9 \pm 1.1$	$59.8 \pm 2.6$

\* EX = exhausted pomace, GSs = grape stalks.

A total sugar conversion of  $69.5 \pm 1.4\%$ mol– $68.4 \pm 1.3\%$ mol was obtained with a 5-HMF yield of  $40.7 \pm 1.2\%$ mol– $40.9 \pm 1.1\%$ mol and selectivity of  $58.6 \pm 2.8\%$ mol– $59.8 \pm 2.6\%$ mol, resulting in very similar activities with respect to the use of pure reagents. Once the robustness was checked, in order to evaluate the stability of the Fe-SMBCs, the catalyst was recovered at the end of the first reaction cycle by using an external magnet and reused for at least five reaction cycles without any significant loss of catalytic activity (Figure 7). No sulfate ions were detected in the reaction mixture after the process [60]. In addition, the acid properties of the catalyst were recovered at the end of the 5<sup>o</sup> cycle of reaction (total acid density =  $0.90 \text{ mmolSO}_3\text{H/g}$ ), which confirms the stability of the catalyst and the absence of leaching during the process.

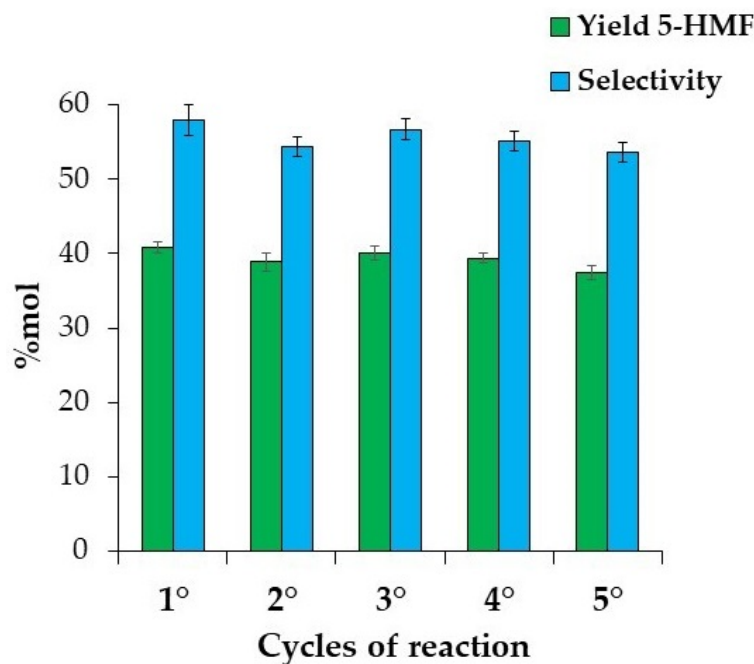


**Figure 7.** Recycling tests of Fe-SMBCs. Reaction conditions: 0.1 g of catalyst, 1 mL of aqueous solution, 2 mL of organic solvent (GVL), 403 K, 3–6 h, 300 rpm.

These results clearly demonstrated that the new procedure of preparing the magnetic sulfonated biochar derived from winery waste allowed us to obtain selective and stable systems for the catalysis of dehydration of fructose to produce 5-HMF. These experimental findings validated the effectiveness of the proposed scheme of valorization of the winery waste, as reported in Figure 1, offering an alternative procedure for the management of grape pomace and stalks, towards a final zero-waste discharge and the concomitant generation of fine chemicals.

#### 2.4. Scaling up of Dehydration Process and Future Perspectives

In order to perform a preliminary study on the feasibility of the dehydration process of simple sugars that are contained in winery waste for the synthesis of 5-HMF, a first evaluation of the methods that are currently used for the isolation of the target product was carried out. In general, thermal evaporation of organic solvents for the recovery of 5-HMF at the end of the dehydration process is not always the most efficient solution. It leads to a partial decrease in the amount of 5-HMF that is produced (recovery yield = 50–70%mol) [40]. The problem of separating 5-HMF has been addressed in several reports, in which a variety of different techniques have been discussed. Reactive distillation under a very high vacuum and temperature (130–150 Pa, 453 K) has been proposed, despite the risk of thermal stability of the 5-HMF, achieving a final recovery greater than 90%mol [61,62]. However, downstream separation and purification of 5-HMF make up most of the costs of the overall production (60–70%). An alternative to distillation is the recovery of 5-HMF from the reaction medium by using adsorbents. Several systems, including zeolites, polymers and resins, have been investigated for the selective adsorption of 5-HMF [63,64]. However, this approach requires further process steps for the recovery of the final product, which leads to an increase in overall costs. For these reasons, the in situ conversion of 5-HMF into more stable and easier-to-isolate chemical compounds is currently the most useful and cost-effective strategy [65]. For example, Motagamwala et al. (2018) [66] reported a process for converting 5-HMF to 2,5-furandicarboxylic acid (2,5-FDCA), a monomer that is used for the production of bio-based polymers [67]. In detail, fructose was dehydrated to 5-HMF in a GVL/H<sub>2</sub>O solvent system and directly oxidized to FDCA over a Pt/C catalyst (yield = 93%mol). Due to its low solubility in the reaction medium (GVL/H<sub>2</sub>O), FDCA was then simply recovered by crystallization, resulting in a 99% pure product. At the same time, useful compounds like 2,5-furandimethanol (2,5-FDM), 2,5-dimethylfuran (2,5-DMF) and 2,5-dimethyltetrahydrofuran (2,5-DMTHF) can be easily obtained by reduction of 5-HMF in the presence of noble metal catalysts (Pt, Ru, Au) and directly used to produce fine chemicals, liquid fuels and polymer materials [68–70]. For these reasons, further studies are being carried out to determine the best strategy for the recovery and conversion of 5-HMF into useful compounds, which will make it possible to define in detail the economic balance of the entire production process.

### 3. Materials and Methods

#### 3.1. Reagents and Instruments

All reagents and solvents used in this work were of analytical grade ( $\geq 99\%$ ) and were used as commercially received from Sigma-Aldrich (St. Louis, MO, USA), without any purification or treatment. Fourier transform infrared spectroscopy (FTIR) experiments were performed by using a FTIR spectrophotometer (Nicolet Summit Thermo Fisher Scientific, Waltham, MA, USA) equipped with an Everest Diamond ATR module. FTIR spectra were recorded in the frequency range of 4000 to 400 cm<sup>-1</sup> at resolution of 4 cm<sup>-1</sup> with 32 scans. Scanning electron microscopy (SEM) and energy-dispersive X-ray (EDX) spectra were carried out by using a tabletop microscope TM4000Plus (Hitachi, Tokyo, Japan). X-ray diffraction (XRD) analysis was conducted by using an Empyrean (Malvern169 Panalytical, Chipping Norton, Australia) diffractometer equipped with a PIXcel1D-Medipix3 detector operating with CuK $\alpha$  radiation (Cu K $\alpha$   $\lambda$  = 1.5406 Å, 45 kV, 40 mA). The data were collected in the range ( $2\theta$ ) of 5–60° and processed with the HighScore Plus software (version 4.8)

and PDF2 database. The N<sub>2</sub> adsorption isotherms were measured with a high-performance adsorption analyzer (ASAP 2020, Micromeritics, Norcross, GA, USA) at the temperature of liquid nitrogen (77 K). The specific surface area was determined by using the Brunauer–Emmett–Teller (BET) method. The pore diameter, volume and distribution were calculated by the NonLocal Density Functional Theory (NLDFT) method from the obtained isotherms. Structural carbohydrates (free simple sugars, EHS and cellulose) were determined by using a GS50 chromatography system (High-Performance Anion-Exchange Chromatography, Dionex-Thermo Fisher Scientific, Sunnyvale, CA, USA) equipped with an AS50 autosampler (Dionex, Sunnyvale, CA, USA), an ED50 pulsed amperometric detector (Dionex, Sunnyvale, CA, USA), with gold electrode and a Carbopac PA10 analytical column (250 mm, 4 mm; Dionex, Sunnyvale, CA, USA). The microfiltered Milli-Q water (Sigma-Aldrich, St. Louis, MO, USA) solutions were injected into the instrument (25 µL loop) and analyzed with a flow rate of 0.5 mL min<sup>-1</sup> of an aqueous 18 mM KOH solution generated by an EG40 Eluent generator (Dionex, Sunnyvale, CA, USA). Organic acids and 5-HMF were quantified through high-performance liquid chromatography (HPLC) analysis by using a JASCO instrument (Easton, MD, USA) equipped with an AS 2055 autosampler (Easton, MD, USA), a UV-150 detector (detection wavelengths 235 and 260 nm, respectively) and a Hi-Plex H column (300 mm, 4 mm; Agilent, Santa Clara, CA, USA). The column was thermostatically controlled at 328 K with a flow rate of 0.6 mL min<sup>-1</sup> of an aqueous 10 mM H<sub>2</sub>SO<sub>4</sub> solution used as a mobile phase.

### 3.2. Winery Waste

Grape pomace and stalks were obtained from white grapes harvested from four different terraces of a winery located in Puglia (southern Italy). First, the stalks were manually separated from the grape berries (destemming) by obtaining two different samples, as shown in Figure 1. Subsequently, the grape berries were washed with deionized water to remove dust and soil particles and mechanically pressed to achieve the separation of grape must and pomace, simulating the traditional winemaking process. At the end of the process, part of the obtained grape pomace and the collected stalks were uniformly distributed on trays and dried in a M80-VF convection oven (MPM Instruments S.r.l, Bernareggio, Italy) at 333 K for 3 days for the determination of Total Solids (TSs). The obtained solids were then milled in a commercial mill (Moulinex, Milano, Italy) and sieved to obtain a particle size of 0.4–0.7 mm. At the same time, the residual grape pomace was collected, and the free simple sugars (e.g., glucose, fructose) recovered by two consecutive extractions with deionized water (weight ratio grape-pomace-to-deionized water of 1-to-1). The extracts were collected together (aqueous stream) and analyzed for the determination of the total carbohydrate content for the next dehydration tests (denoted as aqueous stream). Finally, the exhausted pomace was recovered after the extraction process, dried and treated following the same procedure previously described for grape pomace and stalks.

### 3.3. Biomass Characterization

The dried biomass that was recovered in the different phases of the vinification process (grape pomace, exhausted pomace and grape stalks) was analyzed in order to determine the main exploitable components. Their average chemical composition in terms of esterifiable lipids, proteins, free simple sugars, EHS, cellulose, lignin and ashes content are reported in Table 1. All experiments were conducted in triplicate, allowing us to calculate the mean value and standard deviations. Details about the protocol used for the chemical characterization of biomass are given below.

#### 3.3.1. Determination of Total Lipids

In a Falcon tube of 50 mL, 4 g of dried sample was placed with 20 mL of hexane. The system was closed and kept at 298 K for 15 min under stirring (300 rpm) in an orbital incubator (Gallenkamp). At the end of the process, a two-phase system was observed, comprising an upper organic phase in which lipids are dissolved and a lower phase of

exhausted biomass. Four consecutive extractions with hexane on the wet residual solids were carried out with the extracts that were recovered and collected together. Finally, the total lipid content was determined by evaporating the organic solvent under vacuum (353 K, 500 mbar, Rotavapor R-205, Büchi Labortechnik AG, Flawil, Switzerland) and accurately weighing the obtained crude lipid extract [71,72].

### 3.3.2. Determination of Structural Carbohydrates and Lignin Content

The residual solids that were recovered after the preliminary extraction of the lipid component with hexane were dried in an oven at 373 K for 24 h. Structural carbohydrates and lignin content were then determined by adopting a modified National Renewable Energy Laboratory (NREL) method for the characterization of raw biomass. Then, 2 g of the dried sample was suspended into 100 mL of 4%wt H<sub>2</sub>SO<sub>4</sub> solution and stirred at room temperature for 1 h. Following this, 2 mL of this suspension was filtered with a Whatman filter (N<sup>o</sup>42), diluted if necessary, and analyzed for the determination of free simple sugars. The suspension was then kept under reflux for 2 h. The resultant cooled solution was filtered, made up to 200 mL with Milli-Q water and analyzed to determine EHS (including hemicellulose, pectin sugars and exopolysaccharides) and protein content (see Section 3.3.3). The solids recovered from the filtration were washed with over 100 mL of Milli-Q water and dried at 378 K for 24 h. The dried solids were weighed and suspended with 5 mL of 72%wt H<sub>2</sub>SO<sub>4</sub> solution at 277 K for 24 h. The resulting solution was then transferred into a 250 mL glass balloon, made up to 100 mL with Milli-Q water and refluxed for another 2 h. The suspension was filtered through a previously weighed filter, made up to 100 mL with Milli-Q water and analyzed for the determination of cellulose content. Finally, filtered solids were thoroughly washed with Milli-Q water, dried at 378 K for 24 h and weighed. Lignin content was determined by the difference between the weight obtained and the respective ashes after the thermal treatment at 823 K for 3 h.

### 3.3.3. Determination of Protein Content

The protein content was determined using a modified Folin–Lowry method based on the complexation of peptides with copper ions under alkaline conditions and subsequent oxidation, resulting in the formation of a colored complex with its maximum adsorption at 660 nm [73]. Specifically, the aqueous solutions that were obtained after the first acid hydrolysis of the dried samples (see Section 3.3.2) were used for spectrophotometric determinations, in which the proteins that were present were completely hydrolyzed and solubilized by thermal treatment (under reflux, 2 h). The following aqueous solutions were prepared for the analysis:

- (i) Solution A: 268 mg/L sodium tartrate dihydrate (C<sub>4</sub>H<sub>4</sub>Na<sub>2</sub>O<sub>6</sub>·2H<sub>2</sub>O), 23.4 g/L sodium carbonate (Na<sub>2</sub>CO<sub>3</sub>) and 4 g/L sodium hydroxide (NaOH);
- (ii) Solution B: 1.56%wt copper sulfate (CuSO<sub>4</sub>);
- (iii) Solution C: volume ratio Solution A-to-Solution B of 100-to-1;
- (iv) Solution D: 50%vol Folin–Ciocalteu reagent

Subsequently, 2 mL of aqueous solution was placed into a glass Pyrex tube of 20 mL containing 10 mL of Solution C and 1 mL of Solution D. The system was closed and stirred at room temperature for 20 min. Finally, the protein content was spectroscopically detected UV–Visible SP8001 (Metertech, Taipei City, Taiwan, Cina) spectrophotometer by using an external calibration curve obtained with bovine serum albumin (BSA) aqueous solutions in the range from 25 to 150 mg/mL.

### 3.3.4. Determination of Ashes

Ashes were determined by weight loss of dried samples (see Section 3.2) obtained after heating in a muffle furnace at 823 K for 3 h.

### 3.4. Synthesis of Iron Sulfonated Magnetic Biochar Catalysts

A multi-step procedure was used for the synthesis of iron-sulfonated magnetic biochar catalysts (Fe-SMBCs). The process diagram describing the different synthetic steps is reported in Figure 1. Firstly, biochar was obtained by pyrolysis of dried biomass (exhausted pomace and grape stalks) at 873 K for 2 h under nitrogen flow (heating rate 10 K min<sup>-1</sup>, Eurotherm tubular furnace). Subsequently, the biochar obtained was subjected to sulfonation treatment. In particular, the carbonaceous material was immersed into concentrated sulfuric acid (95–98%wt, 1 g solid/10 mL H<sub>2</sub>SO<sub>4</sub>) and kept at 423 K for 10 h under stirring (300 rpm) in a Teflon-lined stainless autoclave. The recovered solid was then filtered, washed with deionized water (until the filtrate was neutral and free of sulfate ions [60]) and dried at 373 K for 15 h. The wet impregnation technique was used to deposit nanometric iron oxide particles on the surface of the sulfonated biochar by using ferric chloride hexahydrate as a precursor. Then, 2 g of sample was suspended in 50 mL of an aqueous solution of FeCl<sub>3</sub>·6H<sub>2</sub>O (weight ratio of Fe-to-biochar 25%) and kept at room temperature for 5 h at 300 rpm. The suspension was then evaporated at 383 K, and the solid was dried at 373 K for 15 h. Finally, Fe-SMBCs were obtained after thermal activation of iron-impregnated biochar at 873 K for 1 h with the formation of Fe<sub>3</sub>O<sub>4</sub> on the surface of the catalysts.

#### Determination of Total Acid Sites

The quantification of the total acid sites of the catalysts and the materials obtained in the different phases of the process (biochar, sulfonated biochar) was determined by Boehm titration method [74]. First, 0.1 of sample was suspended into 10 mL of deionized water, and after 10 min of stirring, the pH of the supernatant solution was measured. The system was then titrated with an aqueous 0.01 M NaOH solution until the neutralization of the supernatant solution was achieved. The total acidity density was calculated as shown in Equation (5):

$$\text{Total acid density (mmol}_{\text{SO}_3\text{H}}/\text{g}) = \frac{C_{\text{NaOH}} \times V_{\text{NaOH}}}{m_{\text{sample}}} \quad (5)$$

where  $C_{\text{NaOH}}$  is the concentration of NaOH,  $V_{\text{NaOH}}$  is the volume of NaOH added and  $m_c$  is the starting amount of sample.

### 3.5. Dehydration Tests

The synthesized catalysts were preliminary tested in the fructose dehydration reaction for the synthesis of 5-HMF. The reactions were carried out in a glass Pyrex reactor of 10 mL with a stopper and a magnetic stirrer. In a typical experimental procedure, 0.1 g of catalyst was mixed with 1 mL of aqueous fructose solution (0.2 mmol) and 2 mL of organic solvent (MIBK or GVL), resulting in a final volume ratio of organic-to-aqueous-phase of 2-to-1. The reactor was closed and placed in a preheated oil bath, maintained at 403 K, and magnetically stirred at 600 rpm for a given reaction time (3, 6 and 12 h). At the end of the process, the system was rapidly cooled in an ice water bath, and the catalyst was recovered using an external magnet to obtain the liquid sample for analysis. The conversion of fructose, the yield and the selectivity of 5-HMF were calculated according to Equations (6)–(8):

$$\text{Fructose conversion (\%mol)} = \frac{\text{mmol}_{\text{starting fructose}} - \text{mmol}_{\text{residual fructose}}}{\text{mmol}_{\text{starting fructose}}} \times 100 \quad (6)$$

$$\text{Yield product (\%mol)} = \frac{\text{mmol}_{\text{product}}}{\text{mmol}_{\text{starting fructose}}} \times 100 \quad (7)$$

$$\text{Selectivity 5-HMF (\%mol)} = \frac{\text{mmol}_{\text{5-HMF}}}{\text{mmol}_{\text{starting fructose}}} \times 100 \quad (8)$$

In the case of MIBK, the partition coefficient (R) of 5-HMF between the two phases (aqueous and organic) was also evaluated by Equation (9).

$$R = \frac{\text{mmol}_{5\text{-HMF organic phase}}}{\text{mmol}_{5\text{-HMF aqueous phase}}} \quad (9)$$

Once the best experimental conditions were identified, the catalysts were finally tested in the dehydration of simple sugars that were present in the water stream and recovered from grape pomace by extraction with water.

#### Reusability of the Catalyst

After each reaction cycle, Fe-SMBCs were recovered by using an external magnet. Then, the catalyst was rinsed thoroughly with water to remove any organic species that were present on the catalyst surface. After drying at 373 K for 15 h, the recovered catalyst was then reused for the next reaction cycle.

#### 4. Conclusions

In this study, a closed-loop strategy for the management and valorization of winery waste was proposed. Starting from grape pomace and stalks, a novel synthetic methodology was developed to obtain iron-sulfonated magnetic biochar catalysts (Fe-SMBCs) after the preliminary recovery of free simple sugars that were present in the winery waste by water extraction. Thanks to their acid and magnetic properties, these catalysts were successfully tested in the dehydration of free simple sugars that were present in the aqueous stream generated for the production of 5-HMF. The application of this innovative and sustainable approach to the management of winery waste will lead not only to a reduction in management costs but also the conversion of waste into a resource, in accordance with the principles of circular economy. Several experimental aspects of this valorisation strategy will be thoroughly studied to achieve better results, and a complete structural characterization of Fe-supported sulfonated biochars will be performed, to elucidate the catalytic potentialities.

**Author Contributions:** Conceptualization, C.P. and L.d.B.; methodology, L.d.B., C.P. and E.S.; validation, L.d.B., C.P. and E.S.; formal analysis, L.d.B., C.P., E.S., H.E.R.-Á., D.I.M.-C., A.M. and M.H.; investigation, L.d.B., C.P., E.S. and M.H.; resources C.P.; data curation, L.d.B. and C.P.; writing—original draft preparation, L.d.B., C.P. and E.S.; writing—review and editing, C.P., L.d.B. and A.B.-P.; supervision, C.P.; project administration, C.P.; funding acquisition, C.P. All authors have read and agreed to the published version of the manuscript.

**Funding:** This work was supported by IPoPBio “Integrated Process and Product Design for Sustainable Biorefineries (MSCA—RISE 2017: Research and Innovation Staff Exchange)”, Project ID: 778168 and “VISION” (PRIN, MIUR, grant 2017FWC3WC).

**Data Availability Statement:** Data are contained within the article.

**Conflicts of Interest:** All authors declare that the research was conducted in the absence of any commercial or financial relationships that could be construed as a potential conflict of interest.

#### References

- World Wine Production Outlook, OIV First Estimates, 7 November 2023. Available online: [https://www.oiv.int/sites/default/files/documents/OIV\\_World\\_Wine\\_Production\\_Outlook\\_2023.pdf](https://www.oiv.int/sites/default/files/documents/OIV_World_Wine_Production_Outlook_2023.pdf) (accessed on 15 January 2023).
- Beres, C.; Costa, G.N.S.; Cabezero, I.; da Silva-James, N.K.; Teles, A.S.C.; Cruz, A.P.G.; Mellinger-Silva, C.; Tonon, R.V.; Cabral, L.M.C.; Freitas, S.P. Towards integral utilization of grape pomace from winemaking process: A review. *Waste Manag.* **2017**, *68*, 581–594. [CrossRef] [PubMed]
- da Costa, B.S.; Muro, G.S.; García, M.O.; Motilva, M.J. Winemaking by-products as a source of phenolic compounds: Comparative study of dehydration processes. *LWT* **2022**, *165*, 113774. [CrossRef]
- Toscano, G.; Riva, G.; Duca, D.; Pedretti, E.F.; Corinaldesi, F.; Rossini, G. Analysis of the characteristics of the residues of the wine production chain finalized to their industrial and energy recovery. *Biomass Bioenergy* **2013**, *55*, 260–267. [CrossRef]

5. Pinto, R.; Correia, C.; Mourão, I.; Brito, L.M. Composting Waste from the White Wine Industry. *Sustainability* **2023**, *15*, 3454. [CrossRef]
6. Niculescu, V.C.; Ionete, R.E. An Overview on Management and Valorisation of Winery Wastes. *Appl. Sci.* **2023**, *13*, 5063. [CrossRef]
7. Flores, S.S. What is sustainability in the wine world? A cross-country analysis of wine sustainability frameworks. *J. Clean. Prod.* **2018**, *172*, 2301–2312. [CrossRef]
8. EUR-Lex. Access to European Union Law. Document 32008R0479. Council Regulation (EC) No 479/2008 of 29 April 2008 on the Common Organization of the Market in Wine, Amending Regulations (EC) No 1493/1999, (EC) No 1782/2003, (EC) No 1290/2005, (EC) No 3/2008 and Repealing Regulations (EEC) No 2392/86 and (EC) No 1493/1999. Available online: <https://eur-lex.europa.eu/legal-content/EN/TXT/?uri=CELEX:32008R0479> (accessed on 15 January 2023).
9. Poblete, R.; Bakit, J. Technical and economical assessment of the treatment of vinasse from Pisco production using the advanced oxidation process. *Environ. Sci. Pollut. Res.* **2023**, *30*, 70213–70228. [CrossRef] [PubMed]
10. Sousa, R.M.O.; Amaral, C.; Fernandes, J.M.; Fraga, I.; Semitela, S.; Braga, F.; Coimbra, A.M.; Dias, A.A.; Bezerra, R.M.; Sampaio, A. Hazardous impact of vinasse from distilled winemaking by-products in terrestrial plants and aquatic organisms. *Ecotoxicol. Environ. Saf.* **2019**, *183*, 109493. [CrossRef]
11. Semitela, S.; Pirra, A.; Braga, F.G. Impact of mesophilic co-composting conditions on the quality of substrates produced from winery waste activated sludge and grape stalks: Lab-scale and pilot-scale studies. *Bioresour. Technol.* **2019**, *289*, 121622. [CrossRef]
12. Cortés, A.; Oliveira, L.F.; Ferrari, V.; Taffarel, S.R.; Feijoo, G.; Moreira, M.T. Environmental assessment of viticulture waste valorisation through composting as a biofertilisation strategy for cereal and fruit crops. *Environ. Pollut.* **2020**, *264*, 114794. [CrossRef]
13. Zacharof, M.P. Grape winery waste as feedstock for bioconversions: Applying the biorefinery concept. *Waste Biomass Valoriz.* **2017**, *8*, 1011–1025. [CrossRef]
14. Muhlack, R.A.; Potumarthi, R.; Jeffery, D.W. Sustainable wineries through waste valorisation: A review of grape marc utilisation for value-added products. *Waste Manag.* **2018**, *72*, 99–118. [CrossRef] [PubMed]
15. Mandade, P.; Gnansounou, E. Potential value-added products from wineries residues. In *Biomass, Biofuels, Biochemicals. Green-Economy: Systems Analysis for Sustainability*; Elsevier: Amsterdam, The Netherlands, 2022; pp. 371–396. [CrossRef]
16. Rodrigues, R.P.; Gando-Ferreira, L.M.; Quina, M.J. Increasing value of winery residues through integrated biorefinery processes: A review. *Molecules* **2022**, *27*, 4709. [CrossRef]
17. Sirohi, R.; Tarafdar, A.; Singh, S.; Negi, T.; Gaur, V.K.; Gnansounou, E.; Bharathiraja, B. Green processing and biotechnological potential of grape pomace: Current trends and opportunities for sustainable biorefinery. *Bioresour. Technol.* **2020**, *314*, 123771. [CrossRef] [PubMed]
18. D'Ambrosio, V.; Martinez, G.; Jones, E.; Bertin, L.; Pastore, C. Ethyl Hexanoate Rich Stream from Grape Pomace: A Viable Route to Obtain Fine Chemicals from Agro by-Products. *Sep. Purif. Technol.* **2023**, *309*, 123100. [CrossRef]
19. Hayrapetyan, G.; Trchounian, K.; Buon, L.; Noret, L.; Pinel, B.; Lagrue, J.; Assifaoui, A. Sequential extraction of high-value added molecules from grape pomaces using supercritical fluids with water as a co-solvent. *RSC Sustain.* **2023**, *1*, 2014–2023. [CrossRef]
20. Licursi, D.; Raspolli Galletti, A.M.; Antonetti, C.; Martinez, G.A.; Jones, E.; Bertin, L.; Di Fidio, N.; Fulignani, S.; Pasini, G.; Frigo, S. Tunable Production of Diesel Bio-Blendstock by Rhenium-Catalyzed Hydrogenation of Crude Hexanoic Acid from Grape Pomace Fermentation. *Catalysts* **2022**, *12*, 1550. [CrossRef]
21. Perra, M.; Leyva-Jiménez, F.J.; Manca, M.L.; Manconi, M.; Rajha, H.N.; Borrás-Linares, I.; Segura-Carretero, A.; Lozano-Sánchez, J. Application of pressurized liquid extraction to grape by-products as a circular economy model to provide phenolic compounds enriched ingredient. *J. Clean. Prod.* **2023**, *402*, 136712. [CrossRef]
22. Rodrigues Machado, A.; Atatoprak, T.; Santos, J.; Alexandre, E.M.; Pintado, M.E.; Paiva, J.A.; Nunes, J. Potentialities of the Extraction Technologies and Use of Bioactive Compounds from Winery By-Products: A Review from a Circular Bioeconomy Perspective. *Appl. Sci.* **2023**, *13*, 7754. [CrossRef]
23. Tapia-Quirós, P.; Montenegro-Landívar, M.F.; Reig, M.; Vecino, X.; Alvarino, T.; Cortina, J.L.; Saurina, J.; Granados, M. Olive mill and winery wastes as viable sources of bioactive compounds: A study on polyphenols recovery. *Antioxidants* **2020**, *9*, 1074. [CrossRef]
24. Chowdhary, P.; Gupta, A.; Gnansounou, E.; Pandey, A.; Chaturvedi, P. Current trends and possibilities for exploitation of Grape pomace as a potential source for value addition. *Environ. Pollut.* **2021**, *278*, 116796. [CrossRef] [PubMed]
25. Yuan, X.; Cao, Y.; Li, J.; Patel, A.K.; Dong, C.D.; Jin, X.; Gu, C.; Yip, A.C.K.; Tsang, D.C.W.; Ok, Y.S. Recent advancements and challenges in emerging applications of biochar-based catalysts. *Biotechnol. Adv.* **2023**, *67*, 108181. [CrossRef]
26. Cheng, F.; Li, X. Preparation and application of biochar-based catalysts for biofuel production. *Catalysts* **2018**, *8*, 346. [CrossRef]
27. di Bitonto, L.; Reynel-Ávila, H.E.; Mendoza-Castillo, D.I.; Bonilla-Petriciolet, A.; Durán-Valle, C.J.; Pastore, C. Synthesis and characterization of nanostructured calcium oxides supported onto biochar and their application as catalysts for biodiesel production. *Renew. Energy* **2020**, *160*, 52–66. [CrossRef]
28. Seow, Y.X.; Tan, Y.H.; Mubarak, N.M.; Kansedo, J.; Khalid, M.; Ibrahim, M.L.; Ghasemi, M. A review on biochar production from different biomass wastes by recent carbonization technologies and its sustainable applications. *J. Environ. Chem. Eng.* **2022**, *10*, 107017. [CrossRef]
29. Ghesti, G.F.; Silveira, E.A.; Guimarães, M.G.; Evaristo, R.B.; Costa, M. Towards a sustainable waste-to-energy pathway to pequi biomass residues: Biochar, syngas, and biodiesel analysis. *Waste Manag.* **2022**, *143*, 144–156. [CrossRef] [PubMed]

30. Merodio-Morales, E.E.; Mendoza-Castillo, D.I.; Bonilla-Petriciolet, A.; Reynel-Avila, H.E.; Milella, A.; di Bitonto, L.; Pastore, C. A novel CO<sub>2</sub> activation at room temperature to prepare an engineered lanthanum-based adsorbent for a sustainable arsenic removal from water. *Chem. Eng. Res. Des.* **2022**, *185*, 239–252. [[CrossRef](#)]
31. Gasim, M.F.; Choong, Z.Y.; Koo, P.L.; Low, S.C.; Abdurahman, M.H.; Suryawan, W.K.; Ho, Y.C.; Lim, J.W.; Oh, W.D. Application of biochar as functional material for remediation of organic pollutants in water: An overview. *Catalysts* **2022**, *12*, 210. [[CrossRef](#)]
32. Kalinke, C.; de Oliveira, P.R.; Bonacin, J.A.; Janegitz, B.C.; Mangrich, A.S.; Marcolino-Junior, L.H.; Bergamini, M.F. State-of-the-art and perspectives in the use of biochar for electrochemical and electroanalytical applications. *Green Chem.* **2021**, *23*, 5272–5301. [[CrossRef](#)]
33. Liu, W.J.; Jiang, H.; Yu, H.Q. Emerging applications of biochar-based materials for energy storage and conversion. *Energy Environ. Sci.* **2019**, *12*, 1751–1779. [[CrossRef](#)]
34. Akhil, D.; Lakshmi, D.; Kartik, A.; Vo, D.V.N.; Arun, J.; Gopinath, K.P. Production, characterization, activation and environmental applications of engineered biochar: A review. *Environ. Chem. Lett.* **2021**, *19*, 2261–2297. [[CrossRef](#)]
35. Leesing, R.; Siwina, S.; Fiala, K. Yeast-based biodiesel production using sulfonated carbon-based solid acid catalyst by an integrated biorefinery of durian peel waste. *Renew. Energy* **2021**, *171*, 647–657. [[CrossRef](#)]
36. Fonseca, J.M.; Spessato, L.; Cazetta, A.L.; da Silva, C.; Almeida, V.D.C. Sulfonated carbon: Synthesis, properties and production of biodiesel. *Chem. Eng. Process. Process Intensif.* **2022**, *170*, 108668. [[CrossRef](#)]
37. Liu, M.; Ye, Y.; Ye, J.; Gao, T.; Wang, D.; Chen, G.; Song, Z. Recent Advances of Magnetite (Fe<sub>3</sub>O<sub>4</sub>)-Based Magnetic Materials in Catalytic Applications. *Magnetochemistry* **2023**, *9*, 110. [[CrossRef](#)]
38. Yi, Y.; Huang, Z.; Lu, B.; Xian, J.; Tsang, E.P.; Cheng, W.; Fang, J.; Fang, Z. Magnetic biochar for environmental remediation: A review. *Bioresour. Technol.* **2020**, *298*, 122468. [[CrossRef](#)]
39. di Bitonto, L.; Scelsi, E.; Errico, M.; Reynel-Ávila, H.E.; Mendoza-Castillo, D.I.; Bonilla-Petriciolet, A.; Corazza, M.L.; Kanda, L.S.R.; Hájek, M.; Stateva, R.P.; et al. A Network of Processes for Biorefining Burdock Seeds and Roots. *Molecules* **2024**, *29*, 937. [[CrossRef](#)]
40. Slak, J.; Pomeroy, B.; Kostyniuk, A.; Grilc, M.; Likozar, B. A review of bio-refining process intensification in catalytic conversion reactions, separations and purifications of hydroxymethylfurfural (HMF) and furfural. *Chem. Eng. J.* **2022**, *429*, 132325. [[CrossRef](#)]
41. Kong, Q.S.; Li, X.L.; Xu, H.J.; Fu, Y. Conversion of 5-hydroxymethylfurfural to chemicals: A review of catalytic routes and product applications. *Fuel Process. Technol.* **2020**, *209*, 106528. [[CrossRef](#)]
42. Zhang, Y.; Zhu, H.; Ji, Z.; Cheng, Y.; Zheng, L.; Wang, L.; Li, X. Experiments and Kinetic Modeling of Fructose Dehydration to 5-Hydroxymethylfurfural with Hydrochloric Acid in Acetone–Water Solvent. *Ind. Eng. Chem. Res.* **2022**, *61*, 13877–13885. [[CrossRef](#)]
43. Zhang, X.; Cui, H.; Li, Q.; Xia, H. High-Yield Synthesis of 5-Hydroxymethylfurfural from Untreated Wheat Straw Catalyzed by FePO<sub>4</sub> and Organic Acid in a Biphasic System. *Energy Fuels* **2023**, *37*, 12953–12965. [[CrossRef](#)]
44. Chen, L.; Xiong, Y.; Qin, H.; Qi, Z. Advances of Ionic Liquids and Deep Eutectic Solvents in Green Processes of Biomass-Derived 5-Hydroxymethylfurfural. *ChemSusChem* **2022**, *15*, e202102635. [[CrossRef](#)]
45. Sampath, G.; Kannan, S. Fructose dehydration to 5-hydroxymethylfurfural: Remarkable solvent influence on recyclability of Amberlyst-15 catalyst and regeneration studies. *Catal. Commun.* **2013**, *37*, 41–44. [[CrossRef](#)]
46. Takagaki, A. Production of 5-hydroxymethylfurfural from glucose in water by using transition metal-oxide nanosheet aggregates. *Catalysts* **2019**, *9*, 818. [[CrossRef](#)]
47. Dibenedetto, A.; Aresta, M.; Pastore, C.; di Bitonto, L.; Angelini, A.; Quaranta, E. Conversion of fructose into 5-HMF: A study on the behaviour of heterogeneous cerium-based catalysts and their stability in aqueous media under mild conditions. *RSC Adv.* **2015**, *5*, 26941–26948. [[CrossRef](#)]
48. Saidi, M.; Safaripour, M.; Ameri, F.A.; Jomeh, M.E. Application of sulfonated biochar-based magnetic catalyst for biodiesel production: Sensitivity analysis and process optimization. *Chem. Eng. Process.-Process Intensif.* **2023**, *190*, 109419. [[CrossRef](#)]
49. Jiang, H.; Dong, X.; Shou, J. Synthesis of Novel Magnetic Carbon Microtube-Based Solid Acid and Its Catalytic Activities for Biodiesel Synthesis. *Catalysts* **2022**, *12*, 305. [[CrossRef](#)]
50. Liu, W.J.; Tian, K.; Jiang, H.; Yu, H.Q. Facile Synthesis of Highly Efficient and Recyclable Magnetic Solid Acid from Biomass Waste. *Sci. Rep.* **2013**, *3*, 2419. [[CrossRef](#)] [[PubMed](#)]
51. Licursi, D.; Galletti, A.M.R.; Bertini, B.; Ardemani, L.; Scotti, N.; Di Fidio, N.; Fulignati, S.; Antonetti, C. Design approach for the sustainable synthesis of sulfonated biomass-derived hydrochars and pyrochars for the production of 5-(hydroxymethyl) furfural. *Sustain. Chem. Pharm.* **2023**, *35*, 101216. [[CrossRef](#)]
52. Xiong, X.; Iris, K.M.; Chen, S.S.; Tsang, D.C.; Cao, L.; Song, H.; Kwon, E.E.; Ok, Y.S.; Zhang, S.; Poon, C.S. Sulfonated biochar as acid catalyst for sugar hydrolysis and dehydration. *Catal. Today* **2018**, *314*, 52–61. [[CrossRef](#)]
53. Gao, W.; Wan, Y.; Dou, Y.; Zhao, D. Synthesis of partially graphitic ordered mesoporous carbons with high surface areas. *Adv. Energy Mat.* **2011**, *1*, 115–123. [[CrossRef](#)]
54. Bedia, J.; Peñas-Garzón, M.; Gómez-Avilés, A.; Rodríguez, J.J.; Belver, C. Review on activated carbons by chemical activation with FeCl<sub>3</sub>. *C* **2020**, *6*, 21. [[CrossRef](#)]
55. da Luz Corrêa, A.P.; Bastos, R.R.C.; da Rocha Filho, G.N.; Zamian, J.R.; da Conceição, L.R.V. Preparation of sulfonated carbon-based catalysts from murumuru kernel shell and their performance in the esterification reaction. *RSC Adv.* **2020**, *10*, 20245–20256. [[CrossRef](#)] [[PubMed](#)]

56. Ngaosuwan, K.; Goodwin, J.G., Jr.; Prasertdham, P. A green sulfonated carbon-based catalyst derived from coffee residue for esterification. *Renew. Energy* **2016**, *86*, 262–269. [[CrossRef](#)]
57. Alonso, D.M.; Wettstein, S.G.; Dumesic, J.A. Gamma-valerolactone, a sustainable platform molecule derived from lignocellulosic biomass. *Green Chem.* **2013**, *15*, 584–595. [[CrossRef](#)]
58. Wu, J.; Yang, R.; Zhao, S.; Chen, W.; Chen, Z.; Chang, C.; Wu, H. Efficient conversion of fructose to produce high-purity 5-hydroxymethylfurfural under low temperature. *Biomass Convers. Biorefin.* **2023**, 1–9. [[CrossRef](#)]
59. Yan, P.; Xia, M.; Chen, S.; Han, W.; Wang, H.; Zhu, W. Unlocking biomass energy: Continuous high-yield production of 5-hydroxymethylfurfural in water. *Green Chem.* **2020**, *22*, 5274–5284. [[CrossRef](#)]
60. Belle-Oudry, D. Quantitative analysis of sulfate in water by indirect EDTA titration. *J. Chem. Edu.* **2008**, *85*, 1269. [[CrossRef](#)]
61. Metkar, P.S.; Till, E.J.; Corbin, D.R.; Pereira, C.J.; Hutchenson, K.W.; Sengupta, S.K. Reactive distillation process for the production of furfural using solid acid catalysts. *Green Chem.* **2015**, *17*, 1453–1466. [[CrossRef](#)]
62. Rachamontree, P.; Douzou, T.; Cheenkachorn, K.; Sriariyanun, M.; Rattanaporn, K. Furfural: A sustainable platform chemical and fuel. *Appl. Sci. Eng. Prog.* **2020**, *13*, 3–10. [[CrossRef](#)]
63. Zheng, J.; Pan, B.; Xiao, J.; He, X.; Chen, Z.; Huang, Q.; Lin, X. Experimental and mathematical simulation of noncompetitive and competitive adsorption dynamic of formic acid–Levulinic acid–5-Hydroxymethylfurfural from single, binary, and ternary systems in a fixed-bed column of SY-01 resin. *Ind. Eng. Chem. Res.* **2018**, *57*, 8518–8528. [[CrossRef](#)]
64. Zhang, Y.B.; Luo, Q.X.; Lu, M.H.; Luo, D.; Liu, Z.W.; Liu, Z.T. Controllable and scalable synthesis of hollow-structured porous aromatic polymer for selective adsorption and separation of HMF from reaction mixture of fructose dehydration. *Chem. Eng. J.* **2019**, *358*, 467–479. [[CrossRef](#)]
65. Jiang, Z.; Zeng, Y.; Hu, D.; Guo, R.; Yan, K.; Luque, R. Chemical transformations of 5-hydroxymethylfurfural into highly added value products: Present and future. *Green Chem.* **2023**, *25*, 871–892. [[CrossRef](#)]
66. Motagamwala, A.H.; Won, W.; Sener, C.; Alonso, D.M.; Maravelias, C.T.; Dumesic, J.A. Toward biomass-derived renewable plastics: Production of 2, 5-furandicarboxylic acid from fructose. *Sci. Adv.* **2018**, *4*, eaap9722. [[CrossRef](#)] [[PubMed](#)]
67. Fei, X.; Wang, J.; Zhang, X.; Jia, Z.; Jiang, Y.; Liu, X. Recent progress on bio-based polyesters derived from 2, 5-furandicarboxylic acid (FDCA). *Polymers* **2022**, *14*, 625. [[CrossRef](#)] [[PubMed](#)]
68. Du, Z.; Yang, D.; Cao, Q.; Dai, J.; Yang, R.; Gu, X.; Li, F. Recent advances in catalytic synthesis of 2, 5-furandimethanol from 5-hydroxymethylfurfural and carbohydrates. *Bioresour. Bioproc.* **2023**, *10*, 52. [[CrossRef](#)]
69. Castillo, C.; Brijaldo, M.H.; Silva, L.P.; Passos, F.B. Recent Advances in Catalytic Conversion of 5-Hydroxymethylfurfural (5-HMF) to 2,5-Dimethylfuran (2,5-DMF): Mechanistic Insights and Optimization Strategies. *ChemCatChem* **2023**, *15*, e202300480. [[CrossRef](#)]
70. Iriondo, A.; Mendiguren, A.; Güemez, M.B.; Requies, J.; Cambra, J.F. 2,5-DMF production through hydrogenation of real and synthetic 5-HMF over transition metal catalysts supported on carriers with different nature. *Catal. Today* **2017**, *279*, 286–295. [[CrossRef](#)]
71. di Bitonto, L.; Scelsi, E.; Locaputo, V.; Mustafa, A.; Pastore, C. Enhancing biodiesel production from urban sewage sludge: A novel industrial configuration and optimization model. *Sustain. Energy Technol. Assess.* **2023**, *60*, 103567. [[CrossRef](#)]
72. di Bitonto, L.; D’Ambrosio, V.; Pastore, C. A novel and efficient method for the synthesis of methyl (R)-10-hydroxystearate and FAMES from sewage scum. *Catalysts* **2021**, *11*, 663. [[CrossRef](#)]
73. Waterborg, J.H. The Lowry Method for Protein Quantitation. In *The Protein Protocols Handbook*; Springer Protocols Handbooks; Walker, J.M., Ed.; Humana Press: Totowa, NJ, USA, 2009. [[CrossRef](#)]
74. Leyva-Ramos, R.; Landin-Rodriguez, L.E.; Leyva-Ramos, S.; Medellin-Castillo, N.A. Modification of corncob with citric acid to enhance its capacity for adsorbing cadmium (II) from water solution. *Chem. Eng. J.* **2012**, *180*, 113–120. [[CrossRef](#)]

**Disclaimer/Publisher’s Note:** The statements, opinions and data contained in all publications are solely those of the individual author(s) and contributor(s) and not of MDPI and/or the editor(s). MDPI and/or the editor(s) disclaim responsibility for any injury to people or property resulting from any ideas, methods, instructions or products referred to in the content.